J. Phys. II France **5** (1995) 1155–1163 AUGUST **1995**, PAGE 1155

Classification
Physics Abstracts
61.30Eb — 67.70Md — 82.70Kj

Discrete Harmonic Model for Stacked Membranes: Theory and Experiment

Ning Lei ([1,2,3,*]), C.R. Safinya ([1,4]) and R.F. Bruinsma ([4,5])

([1]) Materials and Physics Departments and the Interdepartmental Program on Biochemistry and Molecular Biology, University of California, Santa Barbara, CA 93106, USA
([2]) Physics Department, Rutgers, The State University of New Jersey, New Brunswick, NJ 08903, USA
([3]) Exxon Research and Engineering Company, Annandale, NJ 08801, USA
([4]) Institute for Theoretical Physics, University of California, Santa Barbara, CA 93106, USA
([5]) Physics Department, University of California, Los Angeles, CA 90024, USA

(Received 16 January 1995, accepted 21 April 1995)

Abstract. — A discrete harmonic (DH) model has been developed which describes the static structure factor of stacked membranes. The (DH) model was used to analyze a synchrotron small-angle X-ray scattering study in stacked membranes. We studied lyotropic lamellar L_α phase samples in a quaternary mixture consisting of thin water layers coated with surfactant sodium dodecyl sulfate (SDS) and cosurfactant (pentanol) molecules, separated by oil. The experiments on highly oriented L_α phase samples covered a large interlayer spacing range from $d = 49.1$ to 255.8 Å produced by dodecane dilution, which considerably exceeded those of previous high resolution synchrotron scattering studies of powder samples. Two significant differences emerge between the (DH) model and the continuum Caillé model description of smectic-A liquid crystals and multilayer membranes. First, whereas the continuum model is necessarily restricted to the vicinity of the Bragg peaks of the structure factor, the discrete nature of the (DH) model allowed us to fit the experimentally measured X-ray structure factor over the full range of wave-vectors and dilutions. This enabled measurements of the membrane bending and multilayer compressibility elastic constants κ and B separately, in contrast to the continuum model which gives a reliable measurement of the product κB. Second, the (DH) model is able to account for the universally observed anomalously large small angle scattering (SAS) in strongly fluctuating dilute fluid multilayer membranes. The (SAS) is shown to contain contributions both due to concentration fluctuations described previously by Porte *et al.* and Nallet *et al.*, and unexpectedly from a divergent thermal-coherent diffraction effect which dominates in single crystal multilayers.

The physical properties of fluid membranes are of great importance for cell biology, but membranes also form a multitude of interesting phases whose study has been the subject of consider-

(*) Present address: James Franck Institute, University of Chicago, Chicago, IL 60637, USA.

able recent interest, in particular, concerning the role of thermal fluctuations [1,2]. Membranes, which are comprised of bilayer sheets of surfactant molecules, can at low surfactant concentrations fluctuate over a range of geometries such as those encountered in the bicontinuous sponge-like structure of the L_3 phase [3]. In the vicinity of the L_3 phase, one usually encounters very dilute but more organized phases which are readily accessible to structural probes. Of particular interest are the membrane fluctuations in the L_α phase which we focus on in this paper.

The L_α phase is a regularly spaced stack of fluid bilayers separated by solvent, as shown in Figure 1. From a symmetry view point, the L_α phase can be considered as a smectic-A (SmA) liquid crystal. Diffraction experiments studying the thermal diffuse scattering (TDS) around the quasi-Bragg peaks of unoriented powder samples [4,5] confirm that the power-law line-shapes of L_α phase materials are well described by the classical Caillé model of Sm-A liquid crystals, which arises from layer undulations around the one-dimensional stacking order [6].

However, high resolution X-ray synchrotron [4,5] and neutron [7,8] scattering measurements showed that there is also a central peak small-angle-scattering (SAS) around the origin in reciprocal space which had not been observed in studies of SmA materials [9,10]. Porte *et al.* [7] suggested that the central peak (SAS) is a specific signature of the L_α phase and that it is due to the increase of *incoherent* layer fluctuations as the layers are separated under dilution. Nallet *et al.* [8], proposed a continuum theory of the L_α phase, treating the surfactant concentration as a second variable to include incoherent fluctuations. They predicted a non-divergent central peak with a Lorentzian line shape.

To understand the precise nature of the central peak (SAS) and the extensive scattering observed between the origin and the first Bragg peak in these strongly fluctuating membrane systems, we decided to begin with a harmonic model description of a stack of membranes as done previously by Caillé [6], but with the important difference of retaining the discrete nature of the system arising from alternating membrane and solvent layers. Within the harmonic approximation, the discrete model gives a description of the static structure factor over the entire wave-vector range between the central peak (SAS) and the first Bragg peak position, and extending to the larger wave-vector range after the first peak. A similar discrete harmonic Hamiltonian has been considered previously by Holyst *et al.* for analyzing X-ray reflectivity from freely suspended smectic-A films [11]. However, they only considered the root-mean-square roughness of a smectic layer and not the full (r-dependent) height-height correlation function needed for the calculation of the complete static X-ray structure factor as we describe later. Ramaswamy *et al.* have also considered a similar Hamiltonian in their description of the dynamics of lyotropic lamellar phases [12].

Concurrent with the modeling work, we used the recently developed technique of producing highly oriented lamellar membrane samples [7,8], to carry out a detailed high resolution small-angle X-ray scattering study. The quaternary mixtures we studied were highly oriented L_α phase samples consisting of thin water layers coated with surfactant sodium dodecyl sulfate (SDS) and cosurfactant (pentanol) molecules, separated by dodecane (top of Fig. 1). The experiments were carried out at the National Synchrotron Light Source (NSLS) at Brookhaven on beam line X-10A. We used a double bounce Ge(111) monochromator and a triple bounce Ge(111) analyzer crystal set at 8 keV to obtain a longitudinal resolution of $\Delta q_z = 0.00016$ Å^{-1} (HWHM). Tight slits set the out-of-plane resolution at $\Delta q_\perp = 0.003$ Å^{-1} (HWHM). The experiments explored a large interlayer spacing range of the L_α phase produced by dodecane dilution which considerably exceeded those of previous high resolution synchrotron scattering studies [4, 5]. Twelve mixtures were studied with the dodecane weight fraction Φ varying between 0.18 and 0.74, which corresponds to the interlayer spacing increasing from $d = 49.1$ to 255.8 Å for a membrane thickness $\delta = 37$ Å. The samples were sealed in thin rectangular

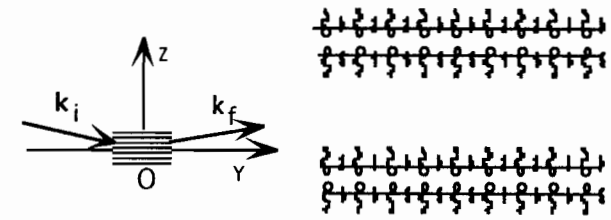

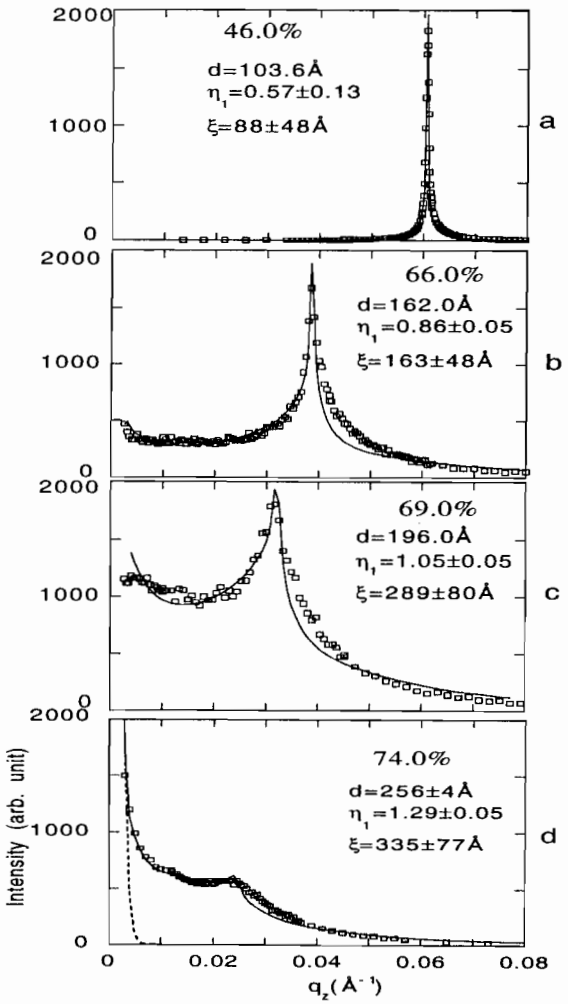

Fig. 1. — Top: Schematic of the multilayer membrane (consisting of water coated with surfactant and cosurfactant) L_α phase with the layers separated by dodecane. Bottom: a) – d): Longitudinal profiles of four mixtures as a function of increasing interlayer spacing (d) resulting from increasing weight fractions of dodecane (% shown in Figure) in the L_α phase covering the small angle and first harmonic wave vector range. Note the dramatic onset of the central peak (centered around $\mathbf{q} = 0$) as d increases in very dilute membranes. The solid lines are fits to the structure factor (Eq. (2)) resulting from the discrete harmonic model Hamiltonian discussed in the text which gave the parameters η_1 and ξ. The mosaic distribution M (HWHM in radians) and the finite size parameters N (number of layers) and the aspect ratio $r = Nd/R$ of the samples were: a) $M = 0.027$, $N = 500$, $r = 0.09$; b) $M = 0.13$, $N = 2000$, $r = 0.07$; c) $M = 0.2$, $N = 1800$, $r = 0.074$; d) $M = 1.8$, $N = 90$, $r = 0.03$. It should be noted here that for low-dimensional systems described by power-law correlations [1,4,5,9], the width of the Bragg peak is normally controlled to a large extent by the exponent η, when $\eta \approx 1$, and not by N.

capillaries ($50 \times 2 \times 0.2$ mm^3) and heat treated. This sample preparation technique [7, 8] resulted in highly oriented lamellar domains with very few defects as verified by polarized light microscopy.

Figure 1 shows the measured X-ray structure factor for oriented L_α samples at increasing levels of dilution. The position of the first Bragg peak at $2\pi/d$, shifts to lower wave-vectors as the layer spacing d increases with increasing dodecane dilution. In Figure 1a (lowest dilution) no central peak (SAS) is visible; in Figure 1b, the first Bragg peak develops asymmetry due to increased small-angle scattering while in Figure 1c the central peak (SAS) grows and finally practically overwhelms the Bragg peak (Fig. 1d).

To interpret these results, we computed the structure factor of the following discrete-harmonic (DH) model Hamiltonian for layer-height fluctuations:

$$2H = \sum_i \int \mathrm{d}^2\mathbf{r} \left(\kappa((\partial^2 x + \partial^2 y)u_i(\mathbf{r}))^2 + B/d(u_{i+1}(\mathbf{r}) - u_i(\mathbf{r}))^2\right) \quad (1)$$

Here, $u_i(\mathbf{r})$ is the undulation displacement of layer i along the z-direction normal to the layers, at a position $\mathbf{r}$ in the (x, y) plane. To allow for finite-size effects, we extended the integral only over a disk of radius R and restricted the layer index to $i = 1, 2, ..., N$. The first term in equation (1) is the Helfrich curvature energy (with bending modulus κ) for symmetric surfactant bilayers [13]. The inter-layer interaction is given by the second term which represents a harmonic restoring potential for the interlayer spacing. B is the interlayer compressibility modulus. Albeit in harmonic form, H allows for both coherent height fluctuations, with $u_i(\mathbf{r})$ slowly varying with i, as well as incoherent fluctuations, with no correlation between $u_i(\mathbf{r})$'s with different index.

The X-ray scattering cross-section is proportional to the product of a single-layer form factor [14] and the structure factor:

$$S(\mathbf{q}) = \sum_{j,j'} \int \mathrm{d}^2\mathbf{r} \int \mathrm{d}^2\mathbf{r}' \mathrm{e}^{iq_z(j-j')d} \mathrm{e}^{i\mathbf{q}_\perp \cdot (\mathbf{r}-\mathbf{r}') - \frac{1}{2}q_z^2 < (u_j(\mathbf{r}) - u_{j'}(\mathbf{r}'))^2 >} \quad (2)$$

For a circular sample of radius R with N layers, this reduces to:

$$\begin{aligned} S(\mathbf{q}) &= 4\pi R^2 \sum_{j=-N,+N} (N - \mid j \mid) \cos(jq_z d) \\ &\times \int_0^{2R} r\mathrm{d}r J_0(q_\perp r) \left(\cos^{-1}(r/2R) - (r/2R)\left[1 - (r/2R)^2\right]^{1/2}\right) \mathrm{e}^{-q_z^2 G_j(\mathbf{r})/2} \end{aligned} \quad (3)$$

with $G_j(\mathbf{r}) \equiv < (u_j(\mathbf{r}) - u_0(0))^2 >$ – the height-height correlation function of the DH model in terms of the parameters η_1 and ξ [15]. The dimensionless parameter $\eta \equiv q_z^2 k_B T/8\pi(\kappa B/d)^{1/2}$ determines the power-law line shape in the Caillé continuum theory [6]. η_n is defined to be the value of η at the n^{th} order Bragg peak $q_z = n2\pi/d$. The parameter $\xi \equiv (\kappa d/B)^{1/4}$, is a correlation length for the fluctuations. For distances greater than ξ, membrane height fluctuations are coherent from layer to layer while for distances less then ξ, fluctuations are single-layer and incoherent [13]. Numerically computed $S(\mathbf{q})$'s were then fitted to the data with N, R, d, η_1 and ξ as fitting parameters. The final structure factor was summed over the sample mosaic distribution which was measured through a standard crystallographic rocking curve. As we mentioned earlier, the same discrete Hamiltonian has been previously employed to calculate the height-squared function $< u_j(\mathbf{r})^2 >$ of freely suspended single crystal smectic

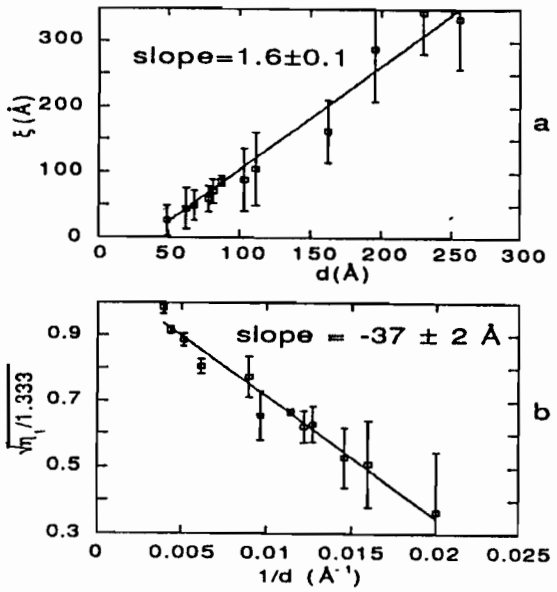

Fig. 2. — Plots of the main parameters (involving the L_α elasticities) ξ and η_1 resulting from fits of the data in the lamellar L_α phase to the structure factor of equation (3). a) The measured length scale $\xi \equiv (\kappa d/B)^{1/4}$ plotted *versus* the interlayer spacing d. The prediction $\xi = (1.39)^{-1/4}(d-\delta)(\kappa/k_BT)^{1/2}$ of the Helfrich theory is shown as a straight line with $\kappa/k_BT = 2.6$; b) the power-law exponent η_1. In the Helfrich theory, $(\eta_1/1.33)^{1/2} = 1 - \delta/d$, which gives a membrane thickness $\delta = 37$ Å. Following the definition of η_1 described in the text, the compressibility elastic constant softens over the dilution range as d increases from 49.1 Å to 255.8 Å with $B = (\pi^2/4\eta_1^2)(k_BT/\kappa)(k_BT/d^3)$.

films [11]. However, the full (**r**-dependent) correlation function $G_j(\mathbf{r})$ described here is needed for analyzing the X-ray structure factor of oriented multilayers with a finite sample mosaic.

The solid lines through the data of Figure 1 result from fits of equation (3) convoluted with the instrumental resolution, to the data. It is immediately clear that *the DH model gives a surprisingly good account of the data for all dilution levels and over the full range of wave-vectors and in particular of the central peak (SAS) scattering*. All previous X-ray analysis had been restricted to the line-shape around the Bragg peaks [4,5]. The η value at the first Bragg peak, η_1, is indicated in Figure 1. These data actually represent the first reliable measurement of the ξ parameter – and thus of the bending rigidity κ – in L_α phase materials by analysis of the scattering profile over the entire wave-vector range. Previous line-shape analysis [4, 5] based on the continuum Caillé model [6], which were necessarily restricted to the vicinity of the Bragg peaks, only gave an accurate measurement of the power-law exponent of the Bragg peaks η_n. The discrete model allows us to fit over the full range of wave-vectors which leads to a measurement of both fitting parameters η_1 and ξ. This, in turn, allows us to measure the elastic constants κ and B separately. We plotted ξ *versus* d in Figure 2a and the results are consistent with the theoretical prediction $\xi = (1.39)^{-1/4}(d-\delta)(\kappa/k_BT)^{1/2}$ of the Helfrich theory [16] with $\kappa/k_BT = 2.6$. Similarly, Figure 2b is consistent with the expected d-dependence of the exponent $\eta_1 = 1.33(1-\delta/d)^2$ when the interlayer interactions are dominated by the so-called Helfrich undulation forces [13], as earlier studies had shown [4,5,7]. Thus, it follows from the definition of η_1 that the compressibility elastic constant over the dilution range from $d = 49.1$ Å to $d = 255.8$ Å softens as $B = (\pi^2/4\eta_1^2)(k_BT/\kappa)(k_BT/d^3)$. The success of the DH model shows

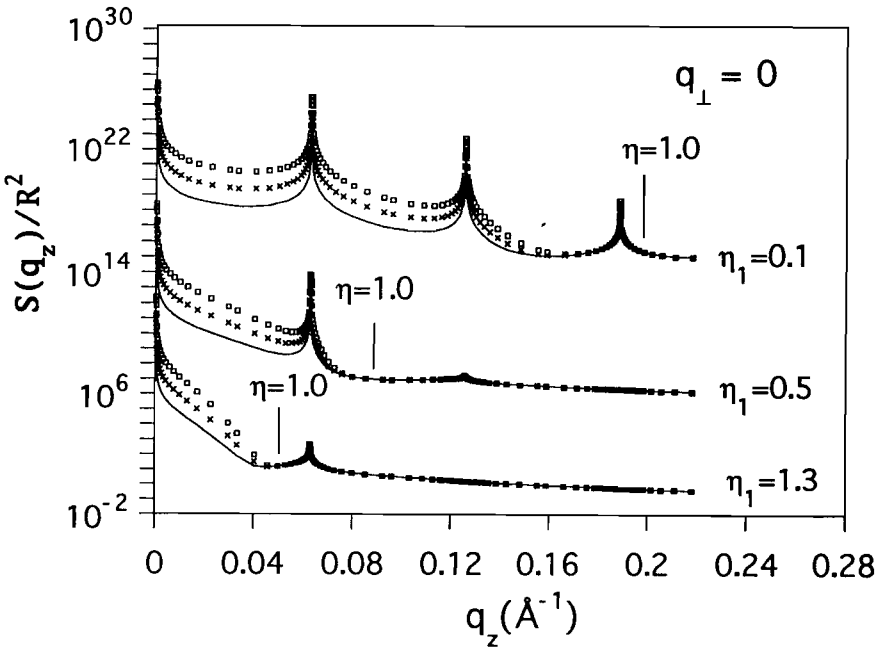

Fig. 3. — Scaling behavior of the numerically computed single crystal structure factor $S(q_z)$ of the DH model as a function of wave vector q_z for three different values of η_1. In each case $N = 2000$, $d = 100$ Å, $\xi = 100$ Å and we chose three different values for the sample radius R ($R/Nd = 2.2$, 9.0, and 35.8 for the solid line, crosses, and squares, respectively). Classical TDS theory predicts that the three sets should collapse on a single curve if we plot the ratio $S(q_z)/R^2$ vs. q_z. The three curves collapse however only for q_z values for which $\eta > 1$. For smaller q_z, $S(q_z)$ increases more rapidly with R than R^2.

that, at least for the present system, dilution of the L_α phase does not introduce significant local L_3 type geometrical disorder in the stacking sequence.

Since the DH model can account for the data including the central peak (SAS), we can study it to better understand the origin of the central peak. To that purpose we show in Figure 3 the structure factor of the DH model for the case of a perfect single crystal with typical parameter values. For conventional continuum TDS, as well as for the Nallet *et al.* model, the structure factor is always proportional to the scattering volume NR^2, away from the immediate vicinity of the Bragg peak positions. In Figure 3 we plot $S(q_z)/R^2$ *versus* q_z for three different R values, so the results should have collapsed onto a single curve. The expected "R^2" scaling is only found for η roughly greater than one. Over the whole range of q_z values for which η is less than one – including the central peak – the structure factor of the DH model clearly does not scale as NR^2. This surprising result is explained as follows. Close to the Bragg peaks, it is possible to evaluate equations (2,3) analytically with the result [17]:

$$S_G(q'_z) \approx C_1(\eta) N R^2 \xi^2 / (q'_z d)^{2-\eta} + C_2(\eta) R^{4-2\eta} \xi^{2\eta} / (q'_z d)^2 \quad (4)$$

assuming $R^2 >> N\xi^2$. Here, $q'_z = q_z - n2\pi/d$ for the n^{th} order Bragg peak while C_1 and C_2 are dimensionless functions of η [17]. The first term of equation (4) is the conventional Caillé power law line-shape with conventional NR^2 scaling [6]. The second term, which is proportional to $R^{4-2\eta}$ rather than R^2, appears because of a divergence in the integrals in equations (2,3) for

$\eta < 1$. Bragg peaks for which $\eta < 1$ are dominated by the new term and thus should show $1/q_z^2$ divergencies rather then the Caillé power law. Examination of the numerical results for the DH model confirms that, for large R, over the whole q_z range for which $\eta < 1$, which includes the central peak region, the structure factor scales as $R^{4-2\eta}/(q_z' d)^2$. The first term in equation (4) produces, in the central peak region, a non-divergent contribution proportional to $NR^2 k_B T/B$ – consistent with the predictions of Nallet *et al.* – but this is overwhelmed by the second term which produces again a R^4/q_z^2 divergence. As we shall see, this second term is mostly important at small q_z in single crystals and becomes progressively suppressed in mosaic and powder samples.

The physical origin of the divergent term is easily understood by noting that a stack of flat layers has a coherent $\mathbf{q} = 0$ Bragg peak with a structure-factor $S_s(q_z, q_\perp = 0) \propto R^4 \sin^2(q_z N d/2)/\sin^2(q_z d/2)$ exhibiting coherent diffraction oscillations. For q_z of order $1/Nd$, $S_s(q_z, q_\perp = 0)$ has the usual finite-size Gaussian line shape but for q_z greater than $1/Nd$, $S_s(q_z, q_\perp = 0)$ is proportional to R^4/q_z^2, and in this range it is likely to overwhelm any standard TDS volume (NR^2) scaling. The second term in equation (4) is simply the finite-temperature analog of $S_s(q_z)$ and we will refer to it as the thermal-coherent contribution. We point out that previous to our work, Gunter *et al.* had also considered finite size effects but only around the first Bragg peak position and not over the entire q_z range [18]. The earlier model calculated the structure factor using the continuum Caillé model of smectic-A liquid crystals. In the vicinity of the first peak of the structure factor where the continuum model is valid, the model gave a similar coherent contribution as the second term in equation (4). In contrast, the DH model is capable of describing the finite size effects over the entire q_z range.

An important consideration regarding the second term in equation(4) has to be noted. The simple analysis of the (SAS) resulting in this term is valid only because of the finite coherence of the X-ray source. For a fully coherent beam extending over the entire sample, the second term produces a central peak which (i) has a strongly diminished small-angle-scattering and (ii) a speckle pattern at finite $\mathbf{q}$ resulting from interference effects between different finite-size lamellar domains. The diminished (SAS) results because for a coherent source at $\mathbf{q} = 0$, the radiation emanating from all the finite-size lamellar domains within the sample, scatter in-phase (or almost in-phase for $q_z << 1/$ (finite-domain-size)), and result in a coherent contribution to the (SAS) which approachs $\delta(\mathbf{q})$-like behavior (i.e., diffraction from an infinite sample) with little tail scattering as the sample volume increases. In the experiments described here, the X-ray source has a finite longitudinal coherence determined by the longitudinal resolution function which is of order 5000 Å and is smaller than the finite size lamellar domains present in these highly oriented preparations. This allowed us to use the random phase approximation in computing the structure factor. We also note that the smallest wave-vector accessed in the (SAS) regime (Fig. 1b-d) q_z (≥ 0.002) was always much larger than the regime $q_z < 1$ /(finite-domain-size), where possible X-ray coherence effects may become apparent.

Our result that the central peak and single crystal Bragg peaks with $\eta < 1$ should be dominated by the thermal-coherent term rather than by the Caillé line shape immediately raises serious problems since there exists a considerable literature of studies for both thermotropic SmA liquid crystals [9,10] and for L_α materials [4,5,7,8] which report Caillé-like line shapes with $\eta < 1$ (including the data shown in Fig. 1). The solution to this difficulty is found by noting that all systems studied to date have been either mosaic [7–10] or powder samples [4,5]. In both cases, the condition $q_\perp = 0$ is not satisfied and the oscillatory factor $J_o(q_\perp r)$ in equations (2,3) tends to suppress the thermal-coherent contribution. Numerical evaluation of the DH structure factor shows that for mosaic samples the higher order Bragg peaks are well described by the Caillé line shape and exhibit standard TDS volume NR^2 scaling. As the mosaic average is performed over a wider angle, more and more lower order Bragg peaks

return to conventional TDS. However, for reasonable values of the mosaic angle, the central peak remains dominated by the thermal-coherent diffraction term. If we use the DH model to fit the experimental data of Fiure 1d and numerically perform the decomposition of the structure factor to extract the thermal-coherent contribution, then we indeed find that the central peak is dominated by thermal-coherent diffraction (dotted line in Fig. 1d) while the first Bragg peaks obey conventional TDS, consistent with previous [4,5,7,8] line-shape analysis of the Bragg peaks. It should be noted that the width of the central peak is large compared to $1/Nd$.

In summary, the DH model can describe the observed X-ray scattering cross-section over the full range of wave vectors for both low and high levels of dilution and it allows direct measurement of the ξ and η_1 parameters, or equivalently the L_α phase elastic moduli κ and B. Single crystals described by the DH model do not exhibit Caillé line-shapes (for $q_\perp = 0$) if $\eta < 1$. The central peak is due to a non-negligible thermal-coherent contribution superimposed on an incoherent contribution due to concentration fluctuations. Our results should be relevant for the X-ray analysis of other well-oriented low-dimensional systems. The reason why the coherent term was previously neglected can be traced to the use of a generally used Gaussian smoothing approximation ("Warren approximation") which facilitates calculation of finite size structure factors like equations (2,3) but which happens to suppress the coherent contribution [19]. Our results show that the Warren approximation may be deceptive when used to analyze the structure factor of oriented systems at their lower critical dimension. Finally, because the DH model is a harmonic model we do not have to consider measure corrections recently considered in other membrane systems [19]. It would be interesting to study the effect of anharmonic "measure" corrections to the DH model [20]. Preliminary estimates show that for the samples studied here they are not important but they must become relevant as we approach the vicinity of a weakly first order L_α-L_3 phase boundary.

Acknowledgments

We have benefited from conversations with T. Lubensky, D. Roux, and S. Milner. We are particularly grateful to A.M. Levelut and S.K. Sinha for illuminating discussions regarding the relationship between the X-ray beam coherence and small-angle-scattering in multilayered systems. One of us (C.R.S.) gratefully acknowledges partial support by NSF under Grant DMR-93-01199, and the Petroleum Research Fund (27837-AC7). A part of this work was completed during the recent Institute of Theoretical Physics Workshop on Biomembranes which is supported by NSF under Grant No. PHY89-04035. The NSLS is supported by the U.S. DOE.

References

[1] See e.g., Lipowsky R., *Nature* **349** (1991) 475; Statistical Mechanics of Membranes and Surfaces, D.R. Nelson, T. Piran, and S. Weinberg, Eds. (World Scientific, Singapore, 1989).

[2] See e.g., Micelles, Membranes, Microemulsions, and Monolayers, A. Ben-Shaul, W. Gelbart and D. Roux, Eds. (Springer-Verlag, New York, 1994).

[3] Porte G., Marignan J., Bassereau P. and May, R., *J. Phys. France* **49** (1988) 511; Cates M. E., Roux D., Andelman D., Milner S. T. and Safran S. A., *Europhys. Lett.* **5** (1988) 733.

[4] Safinya C. R. *et al.*, *Phys. Rev. Lett.* **57** (1986) 2718; Safinya C. R., Sirota E. B., Roux D. and Smith G. S., *Phys. Rev. Lett.* **62** (1989) 1134.

[5] Roux D. and Safinya C. R., *J. Phys. France* **49** (1988) 307.

[6] Caillé A., *C.R. Acad. Sci. Ser. B* **274** (1972) 891.

[7] Porte G., *et al.*, *Europhys. Lett.* **7** (1988) 713.

[8] Nallet F., Roux D. and Milner S.T., *J. Phys. France* **51** (1990) 2333.

[9] Als-Nielsen J., *et al.*, *Phys. Rev. B* **22** (1980) 312; Kaganer V.M., Ostrovskii B.I. and de Jeu W.H., *Phys. Rev. A* **44** (1991) 8158.

[10] Nachaliel E., Keller E. N., Davidov D. and Boeffel C., *Phys. Rev. A* **43** (1991) 2897.

[11] Holyst R., Tweet D.J. and Sorensen L.B., *Phys. Rev. Lett.* **65.**(1990) 2153.

[12] Ramaswamy S., Prost J., Cai W. and Lubensky T. C., *Europhys. Lett.* **23** (1993) 271; Ramaswamy S., Prost J. and Lubensky T.C., *Europhys. Lett.*, in press.

[13] Helfrich W., *Z. Naturforsch.* **33a** (1978) 305.

[14] The single layer form factor considered was the Fourier transform of a simple square density wave with the membrane thickness δ fixed at the expected value $\delta = \varphi_m d$ (where φ_m is the known volume fraction of the membrane). We note that the form factor (which has a first minimum near $2\pi/\delta$) is a smooth decreasing function in the small-angle regime where the structure factor is analysed.

[15] The height-height correlation function for the discrete harmonic model used in the numerical work was (see Ref. [17]):

$G_j(\mathbf{r}) = \eta_1 d^2/(2\pi^2) \int_0^\infty \mathrm{d}x/(x(1+x^2)^{1/2})\{1 - J_0((2x)^{1/2} \mid \mathbf{r} \mid /\xi) \left[(1+x^2)^{1/2} - x\right]^{2|j|}$.

[16] This follows from the definition of ξ and the prediction of the Helfrich theory (Ref. [13]) that the interlayer compressibility $B = 1.39(k_B T)^2 d/[\kappa(d-\delta)^4]$.

[17] Lei Ning, Ph.D. Thesis, Physics Department, Rutgers, The State University of New Jersey (1993); Lei N., Safinya C.R. and Bruinsma R.F., submitted to *Phys. Rev. E.*

[18] Gunter L., Imry Y. and Lajzerowicz J., *Phys. Rev. A* **22** (1980) 1733.

[19] Dutta P. and Sinha S. K., *Phys. Rev. Lett.* **47** (1981) 50.

[20] Cai W., Lubensky T. C., Nelson P. and Powers T., *J. Phys. II France* **4** (1994) 931.